



# Sensitivity of Shipborne GNSS Troposphere Retrieval to Processing Parameters

Aurélie Panetier, Pierre Bosser, Ali Khenchaf

## ► To cite this version:

Aurélie Panetier, Pierre Bosser, Ali Khenchaf. Sensitivity of Shipborne GNSS Troposphere Retrieval to Processing Parameters. International Association of Geodesy Symposia, Springer, pp 1-7, 2022, 10.1007/1345\_2022\_177 . hal-03834685

**HAL Id: hal-03834685**

**<https://hal.science/hal-03834685>**

Submitted on 30 Oct 2022

**HAL** is a multi-disciplinary open access archive for the deposit and dissemination of scientific research documents, whether they are published or not. The documents may come from teaching and research institutions in France or abroad, or from public or private research centers.

L'archive ouverte pluridisciplinaire **HAL**, est destinée au dépôt et à la diffusion de documents scientifiques de niveau recherche, publiés ou non, émanant des établissements d'enseignement et de recherche français ou étrangers, des laboratoires publics ou privés.



Distributed under a Creative Commons Attribution| 4.0 International License

# Sensitivity of Shipborne GNSS Troposphere Retrieval to Processing Parameters

Aurélie Panetier , Pierre Bosser, and Ali Khenchaf

## Abstract

Water vapor is a key variable in meteorology and climate studies. Since the late 90s, Global Navigation Satellite System (GNSS) estimates from ground antennas are commonly used for its description. Indeed, propagation delays are due to the transit of the signal through the atmosphere. The correction of these delays is a crucial step that is needed for the precise GNSS positioning. Integrated Water Vapor (IWV) contents are derived from these delays and are used to describe the distribution of water vapour in the atmosphere.

However, severe meteorological phenomena often originate over the oceans and could strongly affect coastal regions. These phenomena are less well described or forecasted because of the small number of observations available in these regions. In this context, the potential of shipborne GNSS measurements has already been highlighted.

This work aims at investigating the impact of some GNSS processing parameters on IWV retrieval from a shipborne antenna in PPP mode. The studied parameters are cutoff angle, random walk of the estimated delays, and observation weighting. Data were collected for 2 months in 2018 by the GNSS antenna of a vessel operating in the Bay of Brest, France. The impact of the parameters is assessed by comparing the shipborne GNSS-derived IWV to the IWV estimated from a close GNSS ground station, and those computed by the ERA5 reanalysis and operational radiosonde profiles from the nearest Météo-France station. The most satisfying parameterization is shown to have Root Mean Squared (RMS) differences of  $0.5 \text{ kg m}^{-2}$ ,  $0.9 \text{ kg m}^{-2}$ , and  $1.2 \text{ kg m}^{-2}$  compared to GNSS ground station, ERA5, and radiosonde respectively. These conclusive results are also confirmed by comparing the GNSS height estimates to the measurements from the Brest tide gauge, with an RMS difference of 4.9 cm.

## Keywords

Climatology · IWV · Meteorology · PPP · Shipborne GNSS

A. Panetier (✉) · A. Khenchaf  
Lab-STICC/PIM UMR 6285 CNRS, ENSTA Bretagne, Brest, France  
e-mail: [aurelie.panetier@ensta-bretagne.org](mailto:aurelie.panetier@ensta-bretagne.org)

P. Bosser  
Lab-STICC/M3 UMR 6285 CNRS, ENSTA Bretagne, Brest, France

## 1 Introduction

Severe meteorological phenomena often originate in the ocean and can strongly affect coastal regions. In order to be able to secure the coastal regions, atmospheric monitoring is required in these areas. The role played by water vapor in atmosphere dynamics is crucial (Bengtsson 2010); its observation is essential but difficult to achieve over the oceans. Indeed, water vapor measurements generally consist

of surface measurements from ships and buoys (Smith et al. 2019). The water vapor column above the oceans can also be retrieved by satellite radiometers, but this technique provides a low spatial and temporal resolution (Kealy et al. 2012).

Since the late 90s, several studies have highlighted the contribution of GNSS measurements from ground antennas in the retrieval of Integrated Water Vapor (IWV) (Bevis et al. 1992; Haase et al. 2003; Bosser et al. 2010; Bock et al. 2013; Mahfouf et al. 2015). Indeed, the GNSS signal propagation through the troposphere is affected by water vapor. The induced propagation delay is computed in the form of the Zenith Total Delay (ZTD). The ZTD is composed of two parts. First, the Zenith Hydrostatic Delay (ZHD), which can be easily computed from the atmospheric pressure at the antenna height. Secondly, the Zenith Wet Delay (ZWD), which is highly variable and has to be estimated in the GNSS analysis (Boehm and Schuh 2013). Then, the IWV can be derived from the ZWD (Bevis et al. 1992). This kind of IWV retrieval is mainly restricted to land areas with ground GNSS antennas. However, shipborne GNSS IWV retrieval could be of great interest to contribute to water vapor description above the oceans. Some recent studies have already conducted shipborne GNSS IWV retrievals (Wang et al. 2019; Bosser et al. 2021; Mannel et al. 2021). They show an agreement with conventionally measured IWV between 1 and 3 kg m<sup>-2</sup> (Bock et al. 2016; Ning et al. 2016). These differences are due to the uncertainties in the GNSS measurement, as well as processing parameters that are chosen into the modelling used for the analysis of the GNSS raw data.

The quality of GNSS IWV retrieval could be affected by multipath, consisting of the reflection of GNSS signal, and the high correlation between the ZWD and the height estimates during the analysis (Elosegui et al. 1995), particularly in kinematic mode where both of them are estimated at every epoch. Some analysis parameters could be tuned in order to mitigate these effects. A high cut-off angle on satellite elevation will reduce the multipath effect; a low value will help to decorrelate ZWD and height estimates. An elevation dependent weighting of observations will also permit to mitigate the multipath. Finally, a suitable choice of the random walk on the ZWD will help the algorithm to decorrelate height and ZWD estimates as well. This study aims at investigating the impact of these GNSS processing parameters on the IWV retrieval from a shipborne GNSS antenna. Here we processed only GPS raw data acquired on the French survey vessel *Panopée*. It was operating in the Bay of Brest during 49 days between March, 30th and May, 17th of 2018.

The datasets used in this study and the data processing will be detailed in Sect. 2. The Sect. 3 will present the results of the height and IWV retrieval from the shipborne GNSS antenna, and their comparison to other water vapor datasets described in Sect. 2. Finally, Sect. 4 will draw conclusions regarding the identification of a configuration that stands out

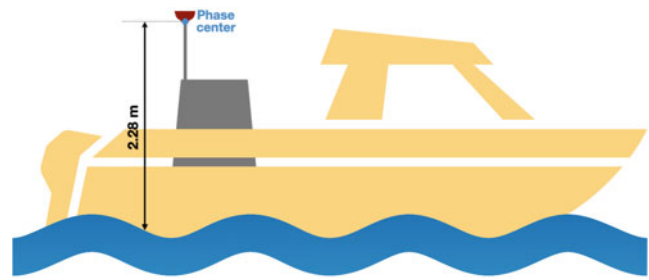


**Fig. 1** Panopée antenna

from the rest of the tested parameters, and will highlight the perspectives.

## 2 Data

### 2.1 Shipborne Antenna Dataset

The GNSS antenna PANO is onboard the French survey vessel *Panopée* operating in the Bay of Brest. The antenna is mounted on a pole located on the echosounder well at the back of the vessel, as illustrated in Fig. 1.

This location was chosen in order to reduce the multipath effects that could affect the antenna, due to the vessel structure. The chosen dataset has a length of 49 days from day 89 to day 137 of year 2018 (March, 30th to May, 17th). During this period, the vessel *Panopée* was operating in the Brest harbor for hydrographic purposes. It was docked more than 90% of the time, leaving for at most a couple of hours straight.

The Gipsy-Oasis II v. 6.4 software (hereafter GIPSY) developed by the Jet Propulsion Laboratory (JPL) of the National Aeronautics and Spatial Agency (NASA), is used to process the PANO dataset (Zumberge et al. 1997). GNSS constellations other than GPS are not supported by GIPSY for kinematic PPP processing with ambiguity resolution (Bertiger et al. 2010), only the GPS data are studied here. The data are processed with a time resolution of 30 s with high-resolution final clocks and orbit products from JPL. To avoid edge effects, it was processed in a 30 h window centered on each day from which the 00–24 h parameters were extracted. The International Earth Rotation and Reference Systems Service (IERS) conventions for solid Earth tides were applied (Petit and Luzum 2010). The Finite Element Solution tide model FES2004 (Lyard et al. 2006) was also applied for ocean tide loading effects, using the coefficients computed by the ocean tide loading provider.<sup>1</sup> The a priori values for ZHD and ZWD, and the coefficients for the mapping functions were extracted from the Technische Universität Wien (TU Wien) VMF database.<sup>2</sup> Three different values, detailed in

<sup>1</sup>Machiel Simon Bos and Hans-Georg Scherneck, <http://holt.oso.chalmers.se/loading/>, last access: 07/09/2021.

<sup>2</sup><https://vmf.geo.tuwien.ac.at/>, last access: 07/09/2021.

**Table 1** Values used for each of the three tested processing parameters. The sin and  $\sqrt{\sin}$  weighting functions of the satellite elevation are applied on the phase observations with a 10 mm uncertainty

Cut-off	Random walk	Weighting
3°	3 mm h <sup>-1/2</sup>	uniform
7°	5 mm h <sup>-1/2</sup>	sin
10°	10 mm h <sup>-1/2</sup>	$\sqrt{\sin}$

Table 1, are tested for each of the three following tested parameters:

- cut-off angle of the satellite elevation, for decreasing the multipath effect and the correlation between ZTD and antenna height estimates;
- random walk on the ZWD modeling, for constraining the ZWD variations to decorrelate ZTD and antenna height estimation;
- satellite elevation weighting on a 10 mm uncertainty for phase observations, for limiting the multipath effect impacting the signal.

The method used to derive the IWV from the ZTD is fully described in Bosser et al. (2021). The IWV is computed from the ZWD with a semi-empirical function using the mean temperature of the air column above the antenna (Bevis et al. 1992). The values for mean temperature were extracted from the TU Wien database.<sup>3</sup> To estimate the wet part, the hydrostatic part must be first computed thanks to the pressure at the antenna height. To that end, the mean sea level pressure retrieved from the European Center for Medium-range Weather Forecasts (ECMWF) fifth ReAnalysis ERA5 is used to compute the ZHD at the mean sea level height according to the Saastamoinen formula (Saastamoinen 1972). The ZHD value is then adjusted with the height difference between the mean sea level and the antenna.

## 2.2 Comparison Datasets

*Reference Ground Based GNSS Antenna* As the vessel Panopée is evolving in the harbor of Brest, it is located close to the Brest ground reference antenna BRST (operated by IGN<sup>4</sup>), with a distance smaller than 10 km. A cut-off angle of 7° with a uniform weighting on phase elevation of 10 mm, and a random walk on the ZWD of 5 kg m<sup>-2</sup> are used to process the BRST data. To stay consistent with the PANO processing, the time resolution is 30 s with high-resolution final satellite products in the GIPSY settings. As BRST is a ground reference station, the data is processed in static PPP mode, in contrast with the kinematic mode used for processing the moving PANO antenna. This processing

strategy has already been applied in many studies (Bock et al. 2016, 2021; Bosser and Bock 2021) and has therefore already been validated.

*Penfeld Tide Gauge* The harbor of Brest houses the Penfeld digital tide gauge operated by the Shom.<sup>5</sup> It provides a reference set of data to qualify the calculation of the PANO antenna height by comparison. It will then be used in order to assess the proper estimation of height and ZTD in the GNSS analysis despite of their strong correlation.

The tide gauge measurement has a 10-min time resolution. Consequently, to compare the PANO height to the tide gauge, we will use the nearest time method. This method consists of taking the PANO height value of the closest time to each tide gauge measurement time.

*ERA5 Reanalysis* The ERA5 reanalysis provided by Copernicus of the ECMWF delivers hourly atmospheric parameters on a 0.25-degree grid all over the Earth (Hersbach et al. 2020). A reanalysis of the water column is directly provided by ERA5 through the so called TCWV product. An extrapolation of the ERA5 value at the location and the height of the PANO antenna is made (Bock et al. 2005) and their IWV are compared by matching the times.

*Radiosonde of Guipavas* Météo-France has a radiosonde station in Brest-Guipavas (less than 20 km from Brest harbor). The sonde data were retrieved from the University of Wyoming sounding archive.<sup>6</sup> The dataset is composed of twice-daily launched sondes measuring the water column in the troposphere.

IWV values are computed by the integration of humidity profiles as proposed in Bock et al. (2021). The radiosonde IWV value is extrapolated to the PANO antenna height as in Bock et al. (2005). Then, the radiosonde IWV is also compared to the PANO IWV by matching the times.

## 3 Qualification of the PANO Results

### 3.1 Antenna Height

First, the PANO height is assessed by comparison to the Brest tide gauge in order to qualify the impact of the choice of the parameterization on the height estimation of the antenna. The vertical lever arm of the shipborne antenna is known with a 1–2 cm accuracy due to the loading of the vessel. The RMS of the difference, varying from 4.9 cm to 6.0 cm depending on the configurations, might be impacted by this uncertainty and should not be used to compare the height

<sup>3</sup><https://vmf.geo.tuwien.ac.at/>, last access: 07/09/2021.

<sup>4</sup><http://rgp.ign.fr/STATIONS/#BRST>, last access : 07/09/2021.

<sup>5</sup><http://dx.doi.org/10.17183/REFMAR>.

<sup>6</sup><http://weather.uwyo.edu/upperair/sounding.html>, last access: 07/09/2021.

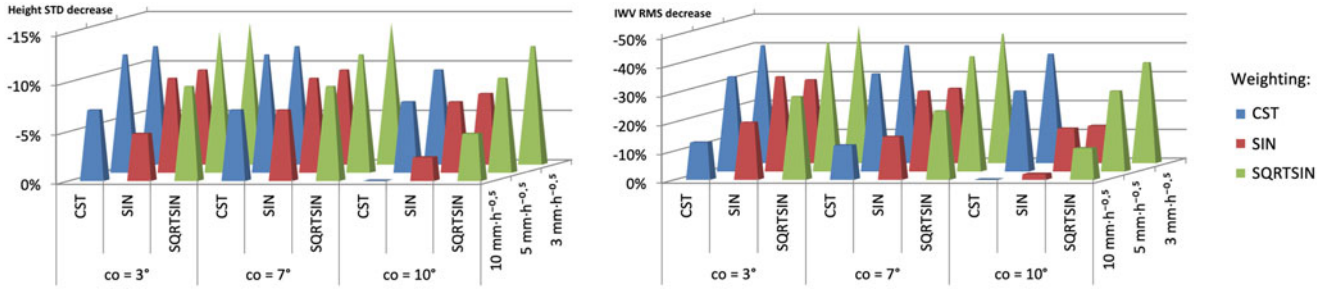


**Fig. 2** Decrease of STD with respect to the worst STD for the PANO height comparison to the Brest tide gauge (left plot) and decrease of RMS with respect to the worst RMS for the PANO IWV comparison to

the ground station BRST IWV (right plot). The highest peaks represent the best configuration as the RMS error or the STD is improved, as the lowest of all the parameterizations

of the PANO antenna with the tide gauge. Therefore, the standard deviations (STD) of the differences are computed for each treatment. The provided STD of the difference in the most unfavorable case is of 4.2 cm. This applies to the configuration of  $10^\circ$  cut-off angle, uniform weighting function of the elevation, and  $10 \text{ mm h}^{-1/2}$  random walk on ZWD. Considering the uncertainty of the vertical lever arm, a STD higher than 4.0 cm is considered to be deteriorating the height estimate. Then, the contribution of each configuration is assessed by computing the decreases of STD with respect to the worst STD value of 4.2 cm. The resulting percentages are shown in Fig. 2 (left).

One can observe here that when parameterizing the PPP processing of the PANO antenna with the sine weighting function (SIN), the STD increases in all configurations. It could be preferred to not use this weighting function, although it gives better results than the uniform function (CST) only in the case of a  $10 \text{ mm h}^{-1/2}$  random walk on the ZWD and  $10^\circ$  cut-off angle. On the other side, the square-root of a sine weighting function (SQRTSIN) gives significantly better results on all configurations, and thereby should be favored. A choice of a  $10 \text{ mm h}^{-1/2}$  random walk on the ZWD systematically gives a worse STD on the difference between PANO and Brest tide gauge than the lower random walk values. Indeed, the decrease of STD compared to the worst resulting STD of the study is mostly lower of 5%, and until 10%, than when using a random walk of  $3 \text{ mm h}^{-1/2}$  or  $5 \text{ mm h}^{-1/2}$ . These two random walk parameters are decreasing the STD of 10 to 14% compared to the worst STD.

With a  $10^\circ$  cut-off angle, the STD of the difference is high in most cases, except when applying a  $3 \text{ mm h}^{-1/2}$  random walk on ZWD. However, this case does not provide a STD as good as the best parameterization that results in a STD of 3.6 cm. Then, the parameter  $3 \text{ mm h}^{-1/2}$  random walk on ZWD might also be left out when used with both previous ones:  $10 \text{ mm h}^{-1/2}$  random walk on the ZWD and  $10^\circ$  cut-off angle.

The three parameters  $10^\circ$  cut-off angle,  $10 \text{ mm h}^{-1/2}$  random walk on the ZWD and sine weighting function,

provide a STD of the height difference at most 12% better than the worst STD of the difference on height between PANO and the Brest tide gauge. On the contrary, using the other parameters always provide a STD of the height difference at least 12% better than the worst case.

Finally, three parameterizations seem to provide a better height estimation. Indeed, it appears that by favoring the square-root of a sine weighting function, both  $3 \text{ mm h}^{-1/2}$  and  $5 \text{ mm h}^{-1/2}$  random walk on the ZWD are giving relevant results with a  $3^\circ$  cut-off angle. Both random walk values are still relevant with a  $7^\circ$  cut-off angle, even if here the choice of  $5 \text{ mm h}^{-1/2}$  random walk on the ZWD gives a slightly poorer result with  $-12\%$  of STD of the height difference against  $-14\%$  in the three other configurations, compared to the worst case. These couples of parameters must be chosen according to the situation as they give really similar results.

### 3.2 Comparison Between PANO and BRST IWV

The shipborne GNSS IWV are compared to the ground GNSS IWV from BRST station. For each configuration, the Root Mean Squared error (RMS) on the difference between the IWV of stations PANO and BRST is computed, as well as the RMS on the difference between the height of the station PANO corrected from the air draft of the vessel, and the tide gauge.

The resulting bias on the IWV is between  $0.03 \text{ kg m}^{-2}$  in the best case and  $0.51 \text{ kg m}^{-2}$  in the worst situation, and the STD is between  $0.52 \text{ kg m}^{-2}$  and  $0.99 \text{ kg m}^{-2}$ . Although these results are already good regarding to the expectations of  $2 \text{ kg m}^{-2}$ , the purpose of the study is to settle whether a parameterization is better than the others. To this end, statistical tests have been purchased, showing that the biases and the variances are significantly different between each processing configuration. The contribution of each configuration is assessed by computing the decreases of RMS with respect to the worst RMS value of  $1.01 \text{ kg m}^{-2}$ . The resulting



percentages are shown in Fig. 2 (right). Actually, the IWV estimation is improved when the height is well estimated in the PPP processing. This was expected because of the strong correlation of ZWD and height estimates in the analysis.

On the one hand, the best resulting RMS on the difference of the IWV is of  $0.53 \text{ kg m}^{-2}$ . It was obtained with a configuration of  $3^\circ$  of cut-off angle, square-root of a sine weighting function of the elevation of the satellites, and  $3 \text{ mm h}^{-1/2}$  random walk on the ZWD. A RMS higher of maximum  $0.15 \text{ kg m}^{-2}$  than this best parameterization is a lowly significant change. The parameters used to provide such a satisfying RMS on the difference of the IWV are chosen among the following:

- cut-off angle of  $3^\circ$  or  $7^\circ$ ;
- uniform or square-root of a sine weighting function;
- random walk on the ZTD of 3 or  $5 \text{ mm h}^{-1/2}$ .

On the contrary, the worst resulting RMS is of  $1.01 \text{ kg m}^{-2}$ , with a configuration of  $10^\circ$  cut-off angle, uniform weighting function of the elevation, and  $10 \text{ mm h}^{-1/2}$  random walk on the ZWD. Figure 2 shows that choosing the sine function for the elevation weighting or  $10^\circ$  of cut-off angle systematically degrades the RMS on the differences of the IWV as well as the differences of the height. The  $10 \text{ mm h}^{-1/2}$  of random walk on the ZWD does not give suitable results either on the RMS of the IWV and the height, except when the chosen cut-off angle is  $3^\circ$  and the weighting function is square-root of a sine.

Moreover, by choosing one of these parameters ( $10^\circ$  cut-off angle,  $10 \text{ mm h}^{-1/2}$  random walk on the ZWD and sine weighting function), the RMS on the difference of the IWV higher of  $0.15 \text{ kg m}^{-2}$  than the best RMS on the difference of IWV between PANO and BRST. This is significantly higher

than the best resulting RMS of  $0.53 \text{ kg m}^{-2}$  with respect to the other configurations introduced above. These parameters are therefore to be avoided to process ZWD from shipborne GNSS antennas.

Finally, three parameterizations seem to provide a globally better water vapor column estimation by shipborne GNSS PANO with respect to ground GNSS station BRST. Indeed, it appears that by favoring square-root of a sine weighting function as for the height estimation, both  $3 \text{ mm h}^{-1/2}$  ( $-48\%$  of RMS) and  $5 \text{ mm h}^{-1/2}$  ( $-45\%$  of RMS) random walk on the ZWD are giving relevant results with a  $3^\circ$  cut-off angle. Both random walk values are still relevant with a  $7^\circ$  cut-off angle, even if the choice of  $3 \text{ mm h}^{-1/2}$  random walk on the ZWD gives a better result with an improvement of  $45\%$  of RMS here. As previously, these couples of parameters give really similar results, so they can be chosen according to the situation.

### 3.3 Comparison of PANO IWV with ERA5 Reanalysis and Radiosonde

The best computed IWV after Sect. 3.2 is the parameterization  $3^\circ$  cut-off angle, square-root of a sine function for elevation weighting, and  $3 \text{ mm h}^{-1/2}$  random walk on the ZWD. The corresponding IWV dataset is compared to the ERA5 reanalysis and the radiosonde of Brest-Guipavas. Superimposing these timeseries with the BRST one provides the top chart in Fig. 3.

This graph reveals a succession of wet (more than  $20 \text{ kg m}^{-2}$ ) and dry (less than  $10 \text{ kg m}^{-2}$ ) episodes for the region. These events are well described by the different

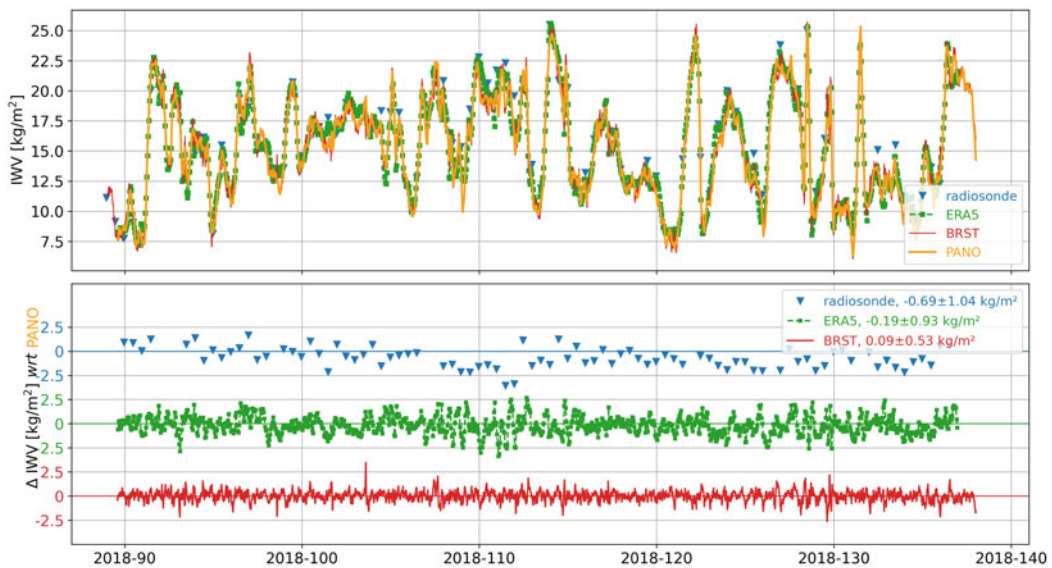


**Fig. 3** Timeseries of the different IWV datasets (top) and differences between the PANO configuration giving the best RMS, and each reference (bottom). Numerical values in bottom figure indicate bias  $\pm$  standard deviation

techniques studied: radiosonde, ERA5 reanalysis from the ECMWF, BRST GNSS permanent station and PANO GNSS station. All over the period of study of nearly 50 days from April to May 2018, these IWV show a very good agreement with each other. The bottom chart on Fig. 3 shows the differences between the IWV estimated with the best PANO processing parameters and the radiosonde of Brest-Guipavas (blue), the ERA5 reanalysis (green) and the BRST GNSS station (red). The mean bias is inferior to  $1 \text{ kg m}^{-2}$  in all cases, but it is negative for ERA5 and radiosonde comparisons. The STD of differences with ERA5 and radiosonde are about  $1 \text{ kg m}^{-2}$ . The difference between PANO and ERA5 is varying from  $2.4 \text{ kg m}^{-2}$  to  $-3.1 \text{ kg m}^{-2}$ . The difference between PANO and the radiosonde is varying from  $1.7 \text{ kg m}^{-2}$  to  $-3.6 \text{ kg m}^{-2}$ . These results are consistent with those presented in recent works (Bosser et al. 2021; Wang et al. 2019) and highlights the potential of retrieving IWV estimates from shipborne GNSS antennas.

## 4 Conclusion

GPS measurements from a shipborne GNSS receiver have been used in order to highlight an adequate parameterization of PPP processing for the improvement of shipborne IWV retrieval. The measurements take place in the harbour of Brest, during 50 days in the second quarter of 2018.

The three processing parameters we focused on here are the cut-off angle for the satellite elevation, the random walk on the ZWD, and the use of different weighting function on the observation phase of the signal. These parameters are commonly modulated to mitigate multipath effects on the signal or correlation between height and ZTD estimates during the analysis.

A best parameterization to process the IWV appears to be  $3^\circ$  cut-off angle with  $3 \text{ mm h}^{-1/2}$  of random walk on the ZWD and square-root of a sine elevation weighting function on the observation phase, in our study. This parameterization provides an IWV difference between the shipborne GNSS antenna and the reference station GNSS antenna of  $0.09 \text{ kg m}^{-2} \pm 0.53 \text{ kg m}^{-2}$ . The comparison of this IWV result with ERA5 and radiosonde provides a difference of  $-0.19 \text{ kg m}^{-2} \pm 0.93 \text{ kg m}^{-2}$  and  $-0.69 \text{ kg m}^{-2} \pm 1.04 \text{ kg m}^{-2}$  respectively. These differences are good according to the literature. GNSS dynamical height computed in the better parameterization case has also been compared to the Brest tide gauge, providing here a difference of  $3.4 \text{ cm} \pm 3.6 \text{ cm}$ . Some parameterizations should be avoided because they systematically give worst results than other parameterizations. Then, the parameters  $10^\circ$  of cut-off angle,  $10 \text{ mm h}^{-1/2}$  of random walk on the ZWD, or sine function of the elevation applied on the phase observation has to be left out of the PPP processing.

In the future, simulations will be conducted for further insight into the role of the parameterization. It will mostly permit to assess whether the use of a sine function for the elevation weighting is systematically degrading the IWV estimation. Results need also to be confirmed with datasets acquired in a broader range of sea states and on a longer period.

**Acknowledgements** We would like to thank the CNRS for supporting this work through the projet GEMMOC in the LEFE/INSU program. We are also grateful to the Fondation Van Allen and Région Bretagne for their financial support, and ENSTA Bretagne for hosting the project.

## Conflict of Interest

The authors declare that they have no conflict of interest.

## Availability of Data and Material

The datasets generated during and/or analysed during the current study are available from the corresponding author on request. Authors' contributions: AP carried out the GNSS data analysis and the comparisons. AP, PB analysed the results and co-wrote the article with contributions from AK.

## References

- Bengtsson L (2010) The global atmospheric water cycle. *Environ Res Lett* 5(2):Article 025202. <https://doi.org/10.1088/1748-9326/5/2/025202>
- Bertiger W, Desai SD, Haines B, Harvey N, Moore AW, Owen S, Weiss JP (2010) Single receiver phase ambiguity resolution with GSP data. *J Geodesy* 84:327–337. <https://doi.org/10.1007/s00190-010-0371-9>
- Bevis M, Bussinger S, Herring TA, Rocken C, Anthes RA, Ware RH (1992) GPS Meteorology: remote sensing of atmospheric water vapor using the Global Positioning System. *J Geophys Res* 97:15787–15801
- Bock O, Keil Ch, Richard E, Flamant C, Bouin M-N (2005) Validation of precipitable water from ECMWF model analyses with GPS and radiosonde data during the MAP SOP. *Q J Roy Meteorol Soc* 131(612):3013–3036. <https://doi.org/10.1256/qj.05.27>
- Bock O, Bosser P, Bourcy T, David L, Goutail F, Hoareau C, Keckhut P, Legain D, Pazmino A, Pelon J, Pipis K, Poujol G, Sarkissian A, Thom C, Tournois G, Tzanos D (2013) Accuracy assessment of water vapour measurements from in situ and remote sensing techniques during the DEMEVAP 2011 campaign at OHP. *Atmos Meas Tech* 6(10):2777–2802. <https://doi.org/10.5194/amt-6-2777-2013>
- Bock O, Bosser P, Pacione, R, Nuret, M, Fourrié N, Parracho A (2016) A high-quality reprocessed ground-based GPS dataset for atmospheric process studies, radiosonde and model evaluation, and reanalysis of HyMeX special observing period. *Quart J Roy Meteorol Soc* 142:56–71. <https://doi.org/10.1002/qj.2701>
- Bock O, Bosser P, Flamant C, Doerflinger E, Jansen F, Fages R, Bony S, Schnitt S (2021) IWV observations in the Caribbean Arc from a

- network of ground-based GNSS receivers during EUREC<sup>4</sup>A. *Earth Syst Sci Data*. <https://doi.org/10.5194/essd-2021-50>
- Boehm J, Schuh H (2013) Atmospheric effects in space geodesy. Springer atmospheric sciences. Springer, Berlin, Heidelberg. <https://doi.org/10.1007/978-3-642-36932-2>
- Bosser P, Bock O (2021) IWV retrieval from ground GNSS receivers during NAWDEX. *Adv Geosci* 55:13–22. <https://doi.org/10.5194/adgeo-55-13-2021>
- Bosser P, Bock O, Thom Ch, Pelon J, Willis P (2010) A case study of using Raman lidar measurements in high-accuracy GPS applications. *J Geodesy* 84:251–265. <https://doi.org/10.1007/s00190-009-0362-x>
- Bosser P, Bock O, Flamant C, Bony S, Speich S (2021) Integrated water vapour content retrievals from ship-borne GNSS receivers during EUREC<sup>4</sup>A. *Earth Syst Sci Data* 13(4):1499–1517. <https://doi.org/10.5194/essd-13-1499-2021ff>
- Elosegui P, Davis JL, Jaldehag RTK, Johansson JM, Niell AE, Shapiro II (1995) Geodesy using the Global Positioning System: The effects of signal scattering on estimates of site position. *J Geophys Res* 100:9921–9934
- Haase J, Ge M, Vedel H, Calais E (2003) Accuracy and variability of GPS tropospheric delay measurements of water vapor in the western Mediterranean. *J Appl Meteor* 42:1547–1568. [https://doi.org/10.1175/1520-0450\(2003\)042](https://doi.org/10.1175/1520-0450(2003)042)
- Hersbach H, Bell B, Berrisford P, Hirahara S, Horányi A, Muñoz-Sabater J, Nicolas J, Peubey C, Radu R, Schepers D, Simmons A, Soci C, Abdalla S, Abellan X, Balsamo G, Bechtold P, Biavati G, Bidlot J, Bonavita M, De Chiara G, Dahlgren P, Dee D, Diamantakis M, Dragani R, Flemming J, Forbes R, Fuentes M, Geer A, Haimberger L, Healy S, Hogan RJ, Hólm E, Janisková M, Keeley S, Laloyaux P, Lopez Ph, Lupu C, Radnoti G, de Rosnay P, Rozum I, Vamborg F, Villaume S, Thépaut J-N (2020) The ERA5 global reanalysis. *Q J Roy Meteorol Soc*. Accepted Author Manuscript. <https://doi.org/10.1002/qj.3803>
- Kealy J, Foster J, Businger S (2012) GPS meteorology: An investigation of ocean-based precipitable water estimates. *J Geophys Res Atmospheres Am Geophys Union (AGU)* 117(D17). <https://doi.org/10.1029/2011jd017422>
- Lyard F, Lefevre F, Letellier T, Francis O (2006) Modelling the global ocean tides: insights from FES2004. *Ocean Dynamics* 56:394–415
- Mahfouf JF, Ahmed F, Moll P, Teferle NF (2015) Assimilation of zenith total delays in the AROME France convective scale model: a recent assessment. *Tellus A* 67:26106. <https://doi.org/10.3402/tellusa.v67.26106>
- Männel B, Zus F, Dick G, Glaser S, Semmling M, Balidakis K, Wickert J, Maturilli M, Dahlke S, Schuh H (2021) GNSS-based water vapor estimation and validation during the MOSAiC expedition. *Atmos Meas Tech* 14:5127–5138. <https://doi.org/10.5194/amt-14-5127-2021>
- Ning T, Wang J, Elgered G, Dick G, Wickert J, Bradke M, Sommer M, Querel R, Smale D (2016) The uncertainty of the atmospheric integrated water vapour estimated from GNSS observations. *Atmos Meas Tech* 9(1):79–92. <https://doi.org/10.5194/amt-9-79-2016>
- Petit G, Luzum B (2010) IERS 2010 conventions, technical report, IERS, Frankfurt-am-Main, Germany
- Saastamoinen J (1972) Atmospheric correction for the troposphere and stratosphere in radio ranging of satellites, in the use of artificial Satellites for geodesy. *Geophysical Monograph* 15, 16:247–251
- Smith SR, Alory G, Andersson A, Asher W, Baker A, Berry DI, Drushka K, Figurskey D, Freeman E, Holthus P, Jickells T, Kleta H, Kent EC, Kolodziejczyk N, Kramp M, Loh Z, Poli P, Schuster U, Steventon E, Swart S, Tarasova O, de la Villéon LP, Vinogradova-Shiffer N (2019) Ship-based contributions to global ocean, weather, and climate observing systems. *Front Marine Sci* 6(434). doi:10.3389/fmars.2019.00434
- Wang J, Wu Z, Semmling M, Zus F, Gerland S, Ramatschi M, Ge M, Wickert J, Schuh H (2019) Retrieving precipitable water vapor from shipborne multi-GNSS observations. *Geophys Res Lett* 46(9). <https://doi.org/10.1029/2019GL082136>
- Zumberge JF, Heflin MB, Jefferson DC, Watkins MM (1997) Precise point positioning for the efficient and robust analysis of GPS data from large networks. *J Geophys Res* 102:5005–5017

**Open Access** This chapter is licensed under the terms of the Creative Commons Attribution 4.0 International License (<http://creativecommons.org/licenses/by/4.0/>), which permits use, sharing, adaptation, distribution and reproduction in any medium or format, as long as you give appropriate credit to the original author(s) and the source, provide a link to the Creative Commons license and indicate if changes were made.

The images or other third party material in this chapter are included in the chapter's Creative Commons license, unless indicated otherwise in a credit line to the material. If material is not included in the chapter's Creative Commons license and your intended use is not permitted by statutory regulation or exceeds the permitted use, you will need to obtain permission directly from the copyright holder.

